Degradation of Phenol by Photocatalysis Using TiO_2/Montmorillonite Composites Under UV Light

Huijuan Li (muzilihuijuan@163.com)
Chemical Engineering ,Southwest forestry University https://orcid.org/0000-0001-5402-9325
Yeting Yao
SWFU: Southwest Forestry University
Xiaoyan Yang
SWFU: Southwest Forestry University
Xusheng Zhou
SWFU: Southwest Forestry University
Ran Lei
SWFU: Southwest Forestry University
Shufang He
Kunming Institute of Technology: Kunming University of Science and Technology

Research Article

Keywords: Montmorillonite, Titanium dioxide, Sol-gel method, Phenol degradation

Posted Date: September 27th, 2021

DOI: https://doi.org/10.21203/rs.3.rs-848926/v1

Abstract

Composites of Titanium (IV) oxide combined with montmorillonite (MMT) with various TiO_2/MMT were prepared for photocatalysis application. The prepared samples were characterized by X-ray diffraction (XRD), transmission electron microscopy (TEM), Fourier transform infrared spectroscopy (FTIR), and diffuse reflectance UV–visible spectroscopy. The main influential factors such as the TiO_2/MMT dose, calcined temperature and pH value of the solution were studied. The main intermediates of phenol degradation were determined by High Performance Liquid Chromatography (HPLC). The results showed that the average size of TiO_2 nanoparticles was decreased from 22.51 nm to 10.66 nm through the immobilization on MMT. The components in the interlayer domain were replaced by titanium pillars, and the pillaring reaction proceeded in the interlayer domain, and the basic skeleton of MMT was unchanged, and also TiO_2 was dispersed on the surface of the MMT. When the initial concentration of phenol is 10 mg/L, the phenol solution pH is 6 and the UV light irradiation time is 240 min, the phenol degradation rate of 30%TiO_2/MMT composite is 89.8%, which is better than MMT (11.5%) and pure TiO_2 (58.8%). It shows that TiO_2 loaded on MMT improves its photocatalytic activity. The phenol reaction process detected by HPLC showed that it had undergone through hydroquinone and benzoquinone, and finally converted into maleic acid and carbon dioxide and small molecules. The possible photocatalysis mechanism is presented.

Introduction

Phenol and its derived compounds are one of the most toxic, and are used widely in petrochemical, chemical, and pharmaceutical industries. When they enter into the natural waters will cause serious pollution and great harm to environment. Drinking water containing phenols may cause severe renal insufficiency, convulsions, and even death (Ruikun Wang 2019). Phenol degradation techniques include adsorption, extraction, electrolysis and photocatalytic oxidation (Lingeswarran Muniandy 2014). Among them, TiO_2-based catalysts can handle with higher concentrations of phenol-containing wastewater, mild reaction conditions, high treatment efficiency and no secondary pollution, and is widely used as photoelectric conversion, photochemical synthesis, and photocatalytic oxidation of environmental pollutants (Paulina Górska 2009; Ali Gundogdu et al. 2012). However, poor adsorption, narrow absorption spectrum and difficult recovery of nanoparticles of TiO_2 limit its application in water treatment (Sreenivasan Koliyat Parayil 2012).

Montmorillonite (MMT) is a layered aluminosilicate mineral, its theoretical molecular formula is $N^{z+}_{\chi/z}M_6{}^{2+}[Si_{8-\chi}Al_\chi]O_{20}(OH)_4{\cdot}nH_2O$. The unit is composed of two layers of silicon-oxygen tetrahedron with a layer of aluminum-oxygen octahedron. It belongs to a 2:1 type structure with swellable hydrous aluminosilicate. The special crystal structure makes montmorillonite have ion exchange capacity and dispersion suspension stability. It possesses layered structures, larger interlayer distance, specific surface area and thermal stability, which can be obtained through physical and chemical methods such as pillaring, insertion replacement and ion exchange (Hassan Ouachtak 2021). Y. X. Liu studied the

commercially available montmorillonite KSF as photoactive reagent and utilized for BPA photodegradation, and found that the BPA degradation increased with the concentration of clays in the range of 0.5 g/L to 5 g/L. The photodegradation rate of BPA is fitted well into the Langmuir-Hinshelwood equation (Y. X. Liu 2008). K. Mogyorósi et al prepared clay mineral intercalated TiO_2 nanoparticles, and found that calcination was not necessary for nanocomposites preparation that had high specific surface areas and well-crystallized anatase contents and thus could be used as an efficient photocatalyst(K. Mogyoro´si 2003). Daimei Chen et al. synthesized TiO_2 pillared montmorillonite and investigated as methylene blue photocatalytic activity, the prepared TiO_2/MMT composites exhibited superior photocatalyic property and the maximum removal efficiency was up to 98% within 90 min (Daimei Chen 2012).

In this paper, TiO_2/MMT composites were prepared by a sol-gel method. The phenol solution was used as model degradation molecular. The effects of TiO_2 loading amount, calcination temperature and solution pH on the degradation of phenol by TiO_2/MMT composites were investigated. FTIR, XRD and SEM techniques were used to characterize the prepared composites.

Experimental

1.1. Materials

The montmorillonite (MMT) was supplied from Xinghe County, Inner Mongolia, China (purity 85%, the major compositions is: SiO_2, 78%; Al_2O_3 ,11.63%; MgO, 3.71%; Fe_2O_3, 2.81% and CaO is 2.03%). $(C_4H_9O)_4Ti$, (CR, Sinopharm Chemical Reagent (Shanghai) Co., Ltd .; The components of MMT are shown in Table.1; Phenol, AR, Chengdu Kelong Chemical Reagent Factory; Sodium Chloride, AR, Chengdu Kelong Chemical Reagent Factory; 4-Aminoantipyrine, CR, Shanghai Qiangshun Chemical Reagent Co., Ltd.; Potassium ferricyanide, CR, Shanghai Qiangshun Chemical Reagent Co., Ltd .;

1.2 Sample preparation

(1) Modification of montmorillonite (MMT)

Montmorillonite (Ca-MMT, 100g) was dispersed into 1000 mL 1.0 mol/L NaCl solution, and stirred for 2 h at 60℃ water bath. Then, the resulting suspension was separated by centrifugation and washed with distilled water until no Cl^- (using 0.1 mol/L $AgNO_3$ test), dried at 110℃ for 24 h, ground, sodium montmorillonite (Na-MMT) can be obtained after 100 mesh.

(2) Preparation of TiO_2

TiO_2 was synthesized through sol-gel method. 5 mL Tetrabutyl titanate was dissolved in 7 mL anhydrous ethanol under vigorous stirring. At the same time, the above solution was dropwise added to a mixture with 15 mL ethanol, 8 mL deionized water and 2 mL acetic acid to make a solution. Under vigorously

stirring conditions, the viscosity of the mixed solution turns more and more and then changed into a sol. The product was aged for 24 h, dried at 110 ℃ for 24h and finally at different temperature for 4h.

(3) Preparation of TiO_2/MMT

The TiO_2 sol was mixed with a certain percent of modified Na-MMT aqueous suspension. In this mixed suspension. The beaker was rinsed with absolute ethanol and thoroughly stirred to prepare TiO_2/MMT. Aging for 24h, the sol was dried at 110℃ for 24 h, and then placed in a muffle furnace (Shanghai Chongming Experimental Instrument Factory) and calcined at a certain temperature (300–600℃) for 4 h, a modified TiO_2/MMT is obtained (named as TiO_2/MMT, which is the mass percentage of TiO_2 and MMT, such as 40% TiO_2/MMT means that the TiO_2 mass is 0.4 and the MMT mass is 1.00).

1.3 Characterization

The as-prepared samples were characterized by different techniques. The crystalline phases of the TiO_2/MMT composites were investigated with X-ray diffraction (XRD, Rigaku D/Max 2000, Cu Kα radiation source with wavelength of λ = 0.15418 at 40 kV and 30 mA). The Fourier transform infrared (FT-IR) spectra were recorded on a Spectrum 100 spectrometer (BRUKER TENSOR27). Transmission electron microscopy (TEM, JEOL LEM-100CXII) and scanning electron microscope (SEM, S-3000N, Hitachi, Japan) was used to observe the microstructure of as-prepared composites. Using $BaSO_4$ as the reflectance sample, the UV–vis diffuse reflectance spectra were recorded with a HITACHI U-3010 spectrometer.

1.4 Photocatalytic degradation of phenol

The photocatalytic activities of the produced TiO_2/MMT composites were measured by degrading phenol. In each experiment, 0.2 g photocatalyst was added to 100 mL solution (10 mg/L, the initial pH is 6, if the pH needs change, adjust with acetic acid and ammonia). of the pollutants and stirred in dark for 30 min in order to reach an adsorption-desorption equilibrium. Then, the suspension was irradiated with a UV light source (300 W, Optima wavelength 365 nm). During the irradiation period, an aliquot of 2.0 mL suspension was collected at regular 30 min intervals, centrifuged to remove the photocatalyst, the aliquots were immediately centrifuged and analyzed using UV–vis spectrometer (UV-1800, Shimadzu).

In order to quantify the evolution of intermediate products, the extinction coefficients of maleic acid (MA), fumaric acid (FA), hydroquinone (HQ), catechol (CC), benzoquinone (BQ), and phenol (PhOH) were measured independently. The concentrations of phenolic compounds were calculated using high performance liquid chromatography (HPLC, PerkinElmer Altus 30) equipped with a Sinochrom ODS-BP column (3.5 μm; 4.6×250 mm) and a 220/240 pump, and also equipped with a Spectra 100 UV–Vis detector to identify the degradation products as an evaluation of the photocatalytic activity of the synthesized TiO_2/MMT composites. A mobile phase composition of methanol / NaH_2PO_4 (with 0.5 mol/L) ratio was 70:30. The mobile phase was delivered at a flow rate of 1.0 mL /min and the detection wavelength was set at 254 nm. The 10 uL solutions were filtered on a 0.45 μm cellulosic filter before injected into the HPLC chromatography.

Results And Discussion

2.1 XRD results$_2$

The XRD pattern of the as-prepared pure MMT, TiO_2 and 30%TiO_2/MMT catalysts are shown in Fig. 1. For pure montmorillonite, the diffraction peak at 2θ = 19.77°,21.85° and 26.76° attribute to the Si-O-Si diffraction peak of Na-montmorillonite, the Si-O-Al and the (101) of quartz, respectively. The original montmorillonite sample (MMT) shows a series of reflections at 2θ = 18.64° with d003 = 0.448 nm and 2θ = 19.77° with d100 = 0.449 nm, respectively. According to the JCPDS card (NO. 00-003-0010), it is corresponding to Na-montmorillonite (Hongjuan Sun 2015). The diffraction peaks of TiO_2 at 2θ = 25.2°, 38.1°, 47.7° and 54.4° correspond to those of anatase (101), (004), (105) and (204), respectively. At the same time, there is a rutile characteristic diffraction peak (2θ = 27.43°) for pure TiO_2(600 ℃, 4 h) and 30%TiO_2/MMT (700 ℃, 4 h) which suggests that the montmorillonite as a carrier can increase TiO_2 phase transition temperature, and make it still anatase phase after calcined at 600 ℃. The positions of the characteristic diffraction peaks of montmorillonite in the 30%TiO_2/MMT composite calcined at different temperatures has no obvious change, and the peak strength is weaker. It can be seen that the introduction of TiO_2 do not change the structure of montmorillonite. The diffraction peaks of TiO_2/MMT at 2θ = 26.76° and 31.02° are obviously weakened or even disappeared compared with the original montmorillonite, which indicates that the original Si-O-Al bond was destroyed, and a new Si-O-Ti bond is constructed after replaced the aluminum ion in the interlayer (Lila Djouadi 2018). The average crystal size of the particles can be estimated from the widths of TiO_2/MMT composites reflections by using the Scherrer formula, d = 0.89·λ/(β·cosθ), where λ (1.5413 Å) is the wavelength, θ is the Bragg angle (°), d is the average crystallite size (nm) and β is the full width at half-maximum. The calculated data of the five TiO_2-based catalysts are followed in Table 2.

Table 2
Crystalline size of TiO_2 in different samples

Sample	d/nm
TiO_2(600℃,4h)	22.51
30%TiO_2/MMT (400℃,4h)	6.61
30%TiO_2/MMT (500℃,4h)	7.68
30%TiO_2/MMT (600℃,4h)	10.66
30%TiO_2/MMT (700℃,4h)	29.50

It can be seen from Table.2, The grain size of TiO_2 reduces from 22.51 nm to 10.66 nm for pure TiO_2 and 30%TiO_2/MMT calcined at 600℃ for 4h, indicating that the particle size of TiO_2 pillared montmorillonite

decreased effectively. And the crystalline size of TiO_2 in 30% TiO_2/MMT composites calcined at different temperatures also gradually increased with the temperature.

2.2 SEM and TEM

Figure 2 shows SEM images of raw montmorillonite (a) and TEM images of pure TiO_2 (b) and 30% TiO_2/MMT (c) composites calcined at 600 ℃ for 4h. The raw montmorillonite shows larger particle aggregates with a flower-like layer structure, the flaky structure is relatively close. For the pure TiO_2, the particles is relatively uniform, with some agglomeration, which may be related to the higher calcination temperature, the particle size is about 19 nm. For the 30% TiO_2/MMT (600℃, 4h) composite, it can be observed the larger platelets and layer structure of montmorillonite clearly. Since the TiO_2 nanoparticles were intercalated, the layer space was enlarged and the structural layers of montmorillonite were separated (R. Djellabi 2014). Although the montmorillonite layers were still largely parallel, they lost long-range order in the c direction after TiO_2 intercalation. Which is consistent with the disappearance of the (001) reflection in the XRD patterns(Ping Zhang 2009). The lattice fringe image of the original montmorillonite sample shows that the structural layers are orderly with a layer space of 2.84 nm. And there are a lot of small aggregates, which are probably broken platelets and agglomerates of TiO_2 crystallites caused by the hydrolysis of surface $Ti(OC_4H_9)_4$ (Boualem Damardji 2008). TiO_2 particle size is about 10 nm by calculation, which is consistent with the data calculated by Scherrer formula in XRD. At the same time, TiO_2 pillared montmorillonite decreases its particle size from 19 nm to 10 nm, while the layered structure of montmorillonite remains unchanged, which also make TiO_2/MMT composites keep good adsorption efficiency of montmorillonite, and then enhance the phenol degradation activity of TiO_2/MMT.

2.3 FT-IR characterization

Figure 3 presents FT-IR spectra of different samples of TiO_2, MMT and TiO_2/MMT dried at 110℃ and calcined at 600 ℃ for 4h, respectively. For the purified MMT, the broad band at 3422 cm^{-1} is due to the stretching vibration of the hydroxyl group and the interlayer water molecules. And the weak peak at 3624 cm^{-1} is attributed to -OH stretching vibration of Al-O-H. Bands at 1645 cm^{-1} and 1468 cm^{-1} are caused by the bending vibration of the hydroxyl group and the interlayer water molecules. The vibration peak at 1079 cm^{-1} is caused by the antisymmetric stretching vibration of Si-O-Si in montmorillonite, which caused by the strong hydration of Ca, Mg and Al plasma strengthens the hydrogen bond between the surface of montmorillonite layer and water, weakens and disappears the band of Si-O bond, resulting in the changing of Si-O and Si-O-Si into a single peak (Ke Chen 2001). Bands at 845 cm^{-1} and 794 cm^{-1} attribute to the bending vibration peak of Mg^{2+}-OH and the hydroxyl vibration of MgAl-OH, respectively. And also bands at 521 cm^{-1}, 474 cm^{-1} and 916 cm^{-1} are suggested to the bending vibration of Si-O-Al, Si-O-Si and octahedral Al-O(OH)-Al in montmorillonite independently. The broad peak at 587 cm^{-1} is attributed to Ti-O bond vibration, which indicates that TiO_2 is amorphous. After TiO_2 modified MMT, interlayer water and hydroxyl increased, which restricted the vibration of structural hydroxyl Al-OH. The

peak at 3621 cm^{-1} lost, and the two peaks at 1021 and 917 cm^{-1} appeared, it shows that the composition of the interlayer of montmorillonite changed after TiO_2 was introduced, and the in-plane stretching vibration peaks of Ti-O-C and Si-O-Si generated (Lingling Yuan 2011; Chihiro Ooka et al. 2003). Also at 796 cm^{-1}, the absorption of the hydroxyl vibration peak of MgAl-OH weakened, which may be related to the removal of hydroxyl as octahedron Ti hydrated ions into the interlayer. At the same time, the strength of 521 cm^{-1} peak in the composite is obviously weakened and widened, which is the superposition of Ti-O and Si-O absorption peaks.

The results show that the strength of Si-O bond is also affected by titanium in lay. For the 30% TiO_2/MMT calcined at 600℃ for 2h, 3422 cm^{-1} and 916 cm^{-1} disappear, while 1468 cm^{-1} peak strength decreases, indicating that interlayer water lost. The vibration peak of Ti-O becomes narrow at 600 cm^{-1}, indicating the TiO_2 crystal phase formed. At the same time, the 1070 cm^{-1} peak of 30% TiO_2/MMT changed into a single peak, which seems that the basic framework of MMT remained unchanged and remained the original structure. For the 30%TiO_2/MMT calcined at different temperatures, it can be seen that the peaks at 3625 cm^{-1}, 1030 cm^{-1} and 845 cm^{-1} gradually disappear, and the peaks of 3431 and 1648 cm^{-1} gradually decrease, which is caused by the evaporation of interlayer water (V. Makrigianni 2015).

2.4 UV-ViS

Figure 4 shows diffuse reflectance UV-Vis spectra of 30% TiO_2/MMT calcined from 400–700℃. It can be seen from the Fig. 4 that the absorption band of pure TiO_2 at 200–400 nm belongs to the electron coordinated by the titanium coordinated oxygen atom to the empty orbit of the central titanium atom, the characteristic absorption formed by $OB_{2p} \rightarrow TiB_{3dB}$ charge transfer, in which the tetrahedron at 248 nm. The characteristic peak of coordination titanium, the absorption peak around 337 nm was the absorption peak of octahedral coordination titanium(Aydin Hassani 2015). The peaks of 30% TiO_2/MMT composites calcined at different temperatures around 433 and 504 nm are Fe-O absorption peaks of Fe_2O_3, because of the used montmorillonite content of 2.8% Fe_2O_3. At the same time, 30% TiO_2/MMT composites calcined at different temperatures have a strong light absorption performance. The value Eg was deliberate from the UV–visible pattern of the titled TiO_2/MMT by extrapolating the line through the k axis and it is exposed in Fig. 4. The wavelength maxima had 409.6 nm (pure TiO_2), 427.1 nm (30%TiO_2/MMT, 400℃), 434.7 nm (30%TiO_2/MMT, 500℃), 418.4nm (30%TiO_2/MMT, 600℃), and 451.5nm (30%TiO_2/MMT, 700℃), respectively. Since the photoabsorption performance of the photocatalyst is positively related to the photocatalytic degradation activity of phenol, it was confirmed that the 30% TiO_2/MMT(600℃,2h) prepared by the sol-gel method has the best photocatalytic activity for phenol degradation.

2.5 Photocatalytic activity

2.5.1 Effect of TiO_2 loading amount on TiO_2/MMT

Figure 5 shows the phenol removal efficiency under UV light over MMT, TiO_2 and different loading of TiO_2 on TiO_2/MMT calcined at 600℃ for 4h. The results showed that the photolysis of phenol in the absence of photocatalyst is only 1.5%, which can be neglected. And the phenol degradation is 11.5% over MMT which shows that MMT has a certain adsorption capacity for phenol solution, but the adsorption activity was very low. It has 58.5% photocatalysis activity over pure TiO_2. Also, for different amount loading of TiO_2/MMT, the results indicated that the photo degradation efficiency of phenol increased with TiO_2 content until 30%TiO_2, then decreased after more TiO_2 loading. Because TiO_2 was the active center of the photocatalytic reaction, when its loading is less, the phenol degradation is low. When the loading of TiO_2 was overdose, photo-generated electrons and holes were generated under light conditions, and the photo-generated electrons and holes recombine to form a composite band, which affects the formation of hydroxyl active groups, reduces the utilization of ultraviolet light, causes degradation efficiency reduced. It was concluded that the photocatalytic activity of 30% TiO_2/MMT composites has the best phenol degradation performance under ultraviolet light.

Theoretically, the adsorption and degradation activity of TiO_2/MMT composites on phenol was the sum of the phenol adsorption on montmorillonite and photodegradation over pure TiO_2. However, it can be seen from the Fig. 5, the phenol adsorption rate of montmorillonite to 11.5% and the degradation rate of TiO_2 was 58.8% after 240 minutes under UV light, the sum of the two was only 70.3%, which is significantly lower than the 30%TiO_2/MMT composite (89.75%). On the one hand, the loading of montmorillonite may increase the crystalline phase transition temperature of TiO_2 to a certain extent; it still maintains the anatase phase structure at 600℃. And also increases the degree of TiO_2 dispersion and makes its particles smaller, which contributed to improving the phenol degradation over TiO_2 /MMT composites(Hongjuan Sun 2015).

2.4.2 Effect of calcined temperature

Figure 6 shows the phenol photocatalytic degradation over 30%TiO_2/MMT composites calcined at different temperatures (from 300 to 700℃). For the 30%TiO_2/MMT composites calcined from 300℃ to 600℃, it can be seen that the degradation rate gradually increased with roasting temperature. When calcined at 600℃, the phenol degradation rate reached 89.75%, but is only 15.08% when the roasting temperature is 700℃, decreased significantly. Therefore, in this catalytic reaction system, the optimal calcination temperature of 30% TiO_2 /MMT photocatalytic composite is 600℃.

2.5.2 The effect of the initial pH

The solution pH is one of the important parameters that can markedly affect the photocatalytic process. In the present work, the effect of the initial pH on the phenol photocatalytic degradation efficiency was studied in the pH range of 2–12 (Fig. 7). In this experiment, acetic acid and ammonia are usually used to adjust the pH value of the solution. The results indicated that the degree of photodegradation efficiency increased with the pH values from 2 to 6 and then decreased. It can be seen from Fig. 7 that the photocatalytic performance of the reaction solution under slightly acidic conditions was significantly

higher than that obtained under slightly alkaline conditions, the pH value will change the interfacial charge of the TiO_2/MMT, thereby changing the dispersion of the particles in the solution, and affecting the adsorption behavior of the montmorillonite matrix on the catalyst surface. In the photocatalyst reaction, the electrons were excited from the valence band to the conduction band, forming electrons (e^-) and holes (h^+). The highly active holes consume OH^- in water during the reaction and oxidize them to have strong oxidative active·OH, then e^- and h^+ undergo redox reactions with substances dispersed in water; As the pH value increases, the concentration of OH^- in the solution sharply increases, then the concentration of · OH increased significantly, the conduction electrons reacted with the adsorbed O_2 to form O_2^-, which could also generate · OH with H_2O, so the degradation efficiency increased with the pH value. However, too high a concentration of · OH will cause a decrease in photocatalytic activity (Chunquan Li 2021). Therefore, the photocatalytic effect was better under suitable pH conditions, which has a high photocatalytic degradation rate under acidic conditions.

2.5.2 The effect of 30%TiO_2/MMT (600℃,4h) dosage

Catalyst dosage is an important parameter in heterogeneous photocatalytic reaction. In order to determine the effect of catalyst dosage on the phenol photodegradation, experiments were carried out by varying the amount of 30%TiO_2/MMT from 0.1 to 0.4 g (Fig. 8). Increasing the amount of photocatalyst from 0.1 g to 0.2 g resulted in increasing the photodegradation efficiency from 42.25–89.96% at the reaction time of 240 min, respectively. By adding the catalyst dosage, promoted the production of reactive species. However, more catalyst dosage would also induce greater aggregation of the catalysts and added the turbidity of the solution, reduce the degree of light penetration through the solution and thereby leading to a reduction in the phenol degradation efficiency. Therefore, 0.2 g 30%TiO_2/MMT photocatalysts is the best amount for phenol photocatalytic reaction(Shivatharsiny Rasalingama 2014).

2.5.3 High performance liquid chromatography -(HPLC) analysis

HPLC was employed to identify the degradation products in order to evaluate the catalytic activities over the pure TiO_2 (600°C, 4 h) and 30% TiO_2/MMT (600°C, 4 h) photocatalysts. Under our experimental conditions, benzoquinone (BQ), hydroquinone (HQ), maleic acid (MA), and fumaric acid (FA) have been identified as intermediates. It should be noted that the four compounds comprising were produced in significant amounts during photocatalytic degradation with the two photocatalysts. For the pure TiO_2, the phenol concentration gradually decreased with the reaction time. It found that the four materials (HQ, BQ, MA and FA) are the main aromatic compounds produced by phenol conversion. The highest concentration of the four materials are detected at 210 min and then decreased gradually, also the MA and FA keep the higher concentration than BQ and HQ, which mightbe caused by the BQ and HQ can turn into MA and FA or the phenol itself will be further converted into maleic acid and fumaric acid, and the residual phenol concentration was 27.17 mg/L after reaction for 420 min. During the phenol

photocatalytic degradation over TiO_2, phenol is gradually degraded in the progress of the reaction, and most of it is directly mineralized into CO_2 and water (Asma Turki 2014).

For the 30% TiO_2/MMT catalyst, with the extension of the photocatalytic reaction time, the phenol concentration in the residual solution decreased significantly. After 420 min reaction, the residual phenol concentration was 9.36 mg/L. Total benzoquinone (HQ), hydroquinone (BQ), maleic acid and fumaric acid (FA + MA) produced by the photocatalytic degradation system of 30%TiO_2/MMT. Compared with the pure TiO_2 system, 30%TiO_2/MMT had more phenol photo-degradation efficiency, and the total amount of intermediate products detected is larger than that in the TiO_2 system. The larger amount of HQ + BQ is due to the higher selectivity of 30%TiO_2/MMT in the phenol conversion. The loading of montmorillonite makes·OH produced by TiO_2 easier to attack the para position of phenol. Hydroquinone is produced and further converted into p-benzoquinone. The amount of butadionic acid (FA + MA) detected in the reaction system of 30%TiO_2/MMT for phenol degradation was higher than that of pure TiO_2. Considering the production of HQ + BQ and FA + MA amount produced in this system, their concentration increased first and then decreased. It is speculated that the reaction course of the montmorillonite loading system may be the rapid phenol mineralization to produce CO_2 + H_2O. The amount of acid produced was small, or is rapidly converted to CO_2 under these catalytic conditions (Xiaobo Wang 2014).

The conversion of phenol calculated by liquid chromatography data was 45.7% (TiO_2) and 81.9% (30%TiO_2/MMT), respectively. It was found that the sum of the carbon content of the intermediate substances was much lower than the degradation rate caused by phenol. It is possible that a large amount of carbon was converted into carbon dioxide, leaving the reaction system. In addition, it can be seen from Fig. 10 that almost all the intermediate products of phenol degradation are converted into small molecular substances. With reference to high-performance liquid reaction data and a large amount of literature, it is concluded that under this experimental condition, the reaction mechanism of phenol degradation may be like this:

The good photocatalytic activity of the 30%TiO_2/MMT composites can be ascribed to the following reasons. The photocatalytic mechanism of 30%TiO_2/MMT composites is showed in Fig. 10. TiO_2 in the interlayer of MMT could increase the surface area of TiO_2/MMT composites,and adding the adsorption efficiency of phenol，thus promoting the photodegradation efficiency of 30%TiO_2/MMT. Secondly, TiO_2 loaded on the surface of MMT and improved its disperse, also enlarged the amount of exposed activates for reactions. When the composite photocatalyst is irradiated by sunlight, the electrons (e^-) in the valence band (VB) of TiO_2 will be excited by energy and transfer to the conduction band (CB) to generate photogenerated electrons, which will generate photogenerated holes (hv^+), Photogenerated holes and electrons will combine with water and dissolved oxygen in water to form superoxide radical ($\cdot O_2^-$) and hydroxyl radical (· OH). The two radicals can oxidize phenol to HQ + HQ, and then convert into FA + MA, and finally mineralize into small molecules of H_2O and CO_2.

Conclusions

1)TiO_2/MMT composites were prepared by sol–gel method. The experiment results indicate 30%TiO_2/MMT (600℃,4h) has relatively higher photocatalytic activities than other catalysts. A certain amount of TiO_2 (TiO_2/MMT = 30%) is highly dispersed on MMT surface, and also TiO_2 can cause the layer silicate of MMT to behave as barriers layer of preventing TiO_2 powders from agglomeration and reduce its particle size from 22.51 to 7.68 nm. Besides, the best photoactivity of 30%TiO_2/MMT composites can be due to its smaller particle size, its layer structure and the red shift of the onset absorption edge in the UV–Visible DRS.

2)The initial concentration of phenol was 10 mg/L, the initial pH of the solution was 6, the amount of catalyst used was 2 g/L, and the ultraviolet irradiation time was 240min. Under the condition of, the degradation rate of phenol was 89.8%. For phenol with an initial concentration of 50 mg/L, the phenol conversion detected by liquid chromatography reached 81.9% at 420 min. The phenol degradation rate was much higher than that of pure TiO_2 (45.7%) under the same conditions, indicating that the loading of montmorillonite significantly enhanced the photocatalytic degradation of phenol by TiO_2.

Declarations

Acknowledgement:

The present study was supported by the Joint Project of Basic Agricultural Research Fund of Yunnan Province (2018FG001-051).

The manuscript does not applicable for ethical approval and consent to participate. This study was supported in part by grants from the Joint Project of Basic Agricultural Research Fund of Yunnan Province (2018FG001-051). And all the authors consent to publish. The authors declare that they have no competing interests. All data generated or analyzed during this study are included in this published article.

The authors' contributions are followed as:

Huijuan Li contributed to the conception of the study and wrote the manuscript;

Yeting Yao contributed significantly to analysis and manuscript preparation

Xiaoyan Yang contributed to make the graphs in the manuscript.

Xusheng Zhou performed the experiment;

Ran Lei performed the data analyses;

Shufang He helped perform the analysis with constructive discussions.

References

1. Gundogdu A, Duran C, Basri Senturk H, Soylak M, Ozdes D, Serencam H, Imamoglu M (2012) Adsorption of Phenol from Aqueous Solution on a Low-Cost Activated Carbon Produced from Tea Industry Waste: Equilibrium, Kinetic, and Thermodynamic Study [J]. Chem Eng Data 57:2733–2743. https://doi.org/10.1021/je300597
2. Aydin Hassani A, Khataee S, Karaca (2015) Photocatalytic degradation of ciprofloxacin by synthesized TiO_2 nanoparticles on montmorillonite: Effect of operation parameters and artificial neural network modeling [J]. J Mol Catal A: Chem 409:149–161. http://dx.doi.org/10.1016/j.molcata.2015.08.020
3. Asma Turki C, Guillard, Frédéric Dappozze, Zouhaier Ksibi ,GillesBerhault, Hafedh Kochkar, Phenol photocatalytic degradation over anisotropic TiO_2 nanomaterials: Kinetic study adsorption isotherms and formal mechanisms [J] (2015) Appl Catal B 163:404–413. http://dx.doi.org/10.1016/j.apcatb.2014.08.010
4. Boualem Damardji HK, Duclaux L, David B (2009) Preparation of TiO_2-pillared montmorillonite as photocatalyst Part I. Microwave calcination, characterisation, and adsorption of a textile azo dye [J]. Appl Clay Sci 44:201–205. . 10.1016/j.clay.2008.12.010
5. Chihiro Ooka H, Yoshida M, Horio K, Suzuki T, Hattori (2003) Adsorptive and photocatalytic performance of TiO_2 pillared montmorillonite in degradation of endocrine disruptors having different hydrophobicity [J]. Appl Catal B 41:313–321. https://doi.org/10.1016/S0926-3373(02)00169-8
6. Li C, Zhu N, Yang S, He X, Zheng S, Sun Z, Dionysios D, Dionysiou, A review of clay based photocatalysts: Role of phyllosilicate mineral in interfacial assembly, microstructure control and performance regulation [J], Chemosphere, 2021 273., 129723, https://doi.org/10.1016/j.chemosphere.2021.129723
7. Chen D, Zhu Q, Zhou F, Deng X, Li F, Synthesis and photocatalytic performances of the TiO_2 pillared montmorillonite [J], Journal of Hazardous Materials,2012, 235–236, 186–193, http://dx.doi.org/10.1016/j.jhazmat.2012.07.038
8. Hassan Ouachtak AE, Guerdaoui RH, Akhouairi S, Haouti RE, Hafid N, Addi AA, Šljukic´ B, Diogo MF, Santos (2021) Mohamed Labd Taha, Highly efficient and fast batch adsorption of orange G dye from polluted water using superb organo-montmorillonite: Experimental study and molecular dynamics investigation. J Mol Liq 335:116560. https://doi.org/10.1016/j.matchemphys.2020.124125
9. Hongjuan S, Peng T, Liu B, Xian H (2015) Effects of montmorillonite on phase transition and size of TiO_2 nanoparticles in TiO_2/montmorillonite nanocomposites [J]. Appl Clay Sci 114:440–446,. http://dx.doi.org/10.1016/j.clay.2015.06.026
10. Hongjuan S, Peng T, Liu B (2015) Haiyang Xian,Effects of montmorillonite on phase transition and size of TiO_2 nanoparticles in TiO_2/montmorillonite nanocomposites [J]. Appl Clay Sci 114:440–446. http://dx.doi.org/10.1016/j.clay.2015.06.026 0169–1317

11. Mogyoro´si K, Dékány I, Fendler JH, Preparation and Characterization of Clay Mineral Intercalated Titanium Dioxide Nanoparticles[J], Langmuir 2003, 19, 2938–2946, https://doi.org/10.1021/la025969a
12. Chen K, Li J, Wang W, Zhang Y, Wang X, Su H (2011) The preparation of vanadium-doped TiO_2–montmorillonite nanocomposites and the photodegradation of sulforhodamine B under visible light irradiation [J]. Appl Surf Sci 257:7276–7285. doi:10.1016/j.apsusc.2011.03.104
13. Lingeswarran Muniandy F, Adam AR, Mohamed E-P, Ng (2014) The synthesis and characterization of high purity mixed microporous/ mesoporous activated carbon from rice husk using chemical activation with NaOH and KOH [J]. Microporous Mesoporous Mater 197:316–323. http://dx.doi.org/10.1016/j.micromeso.2014.06.020
14. Lila Djouadi H, Khalaf HB, Boutoumi H, Kezzime A, Arturo Santaballa J, Canle M (2018) Degradation of aqueous ketoprofen by heterogeneous photocatalysis using Bi_2S_3/TiO_2–Montmorillonite nanocomposites under simulated solar irradiation [J]. Appl Clay Sci 166:27–37. https://doi.org/10.1016/j.clay.2018.09.008
15. Yuan L, Huang D, Guo W, Yang Q, Yu J, TiO2/montmorillonite nanocomposite for removal of organic pollutant [J], Appl Clay Sci, 2011, 53, 272–278. doi:10.1016/j.clay.2011.03.013
16. Ping Zhang Z, Mo L, Han X, Zhu B, Wang C, Zhang, Preparation and Photocatalytic Performance of Magnetic TiO_2/Montmorillonite/Fe_3O_4 Nanocomposites [J], Ind Eng Chem Res 2014, 53, 8057–8061, http: //dx.doi.org/10.1021/ie5001696
17. Paulina Górska A, Zaleska J, Hupka (2009) Photodegradation of phenol by UV/TiO_2 and Vis/N, C-TiO_2 processes: Comparative mechanistic and kinetic studies [J]. Sep Purif Technol 68:90–96. https://doi.org/10.1016/j.seppur.2009.04.012
18. Ruikun Wang Q, Ma Z, Zhao X, Ye Q, Jin, Zhenghui Zhao,Ji Liu, Adsorption of Surfactants on Coal Surfaces in the Coking Wastewater Environment: Kinetics and Effects on the Slurrying Properties of Coking Wastewater–Coal Slurry [J], Ind Eng Chem Res 2019, 58, 28, 12825–12834, https://doi.org/10.1021/acs.iecr.9b01829
19. Djellabi R, Ghorab MF, Cerrato G, Morandi S, Gatto S, Oldani V, Di Michele A, Bianchi CL (2014) Photoactive TiO_2–montmorillonite composite for degradation of organic dyes in water [J]. J Photochem Photobiol A 295:57–63. https://doi.org/10.1016/j.jphotochem.2014.08.017
20. Parayil SK, Kibombo HS, Wu C-M, Peng R, Jonas Baltrusaitis b, Ranjit T. Koodali. Enhanced photocatalytic water splitting activity of carbon-modified TiO_2 composite materials synthesized by a green synthetic approach [J]. Int J Hydrogen Energy, 2012, 37, 8257–8267. https://doi.org/10.1016/j.ijhydene.2012.02.067
21. Shivatharsiny Rasalingama HS, Kibombo C-M, Wu R, Peng J, Baltrusaitis, Ranjit T, Koodali. Competitive role of structural properties of titania–silica mixed oxides and a mechanistic study of the photocatalytic degradation of phenol [J]. Appl Catal B, 2014, 148–149, 394–405, http://dx.doi.org/10.1016/j.apcatb.2013.11.025

22. Makrigianni V, Giannakas A, Daikopoulos C, Deligiannakis Y, I. Konstantinou, Preparation, characterization and photocatalytic performance of pyrolytic-tire-char/TiO_2 composites, toward phenol oxidation in aqueous solutions, Applied Catalysis B: Environmental, 2015, 174, 244–252, http://dx.doi.org/10.1016/j.apcatb.2015.03.007
23. Wang X, Huang S, Zhu L, Tian X, Li S, Tang H, Correlation between the adsorption ability and reduction degree of graphene oxide and tuning of adsorption of phenolic compounds [J] (2014) Carbon 69:101–112. http://dx.doi.org/10.1016/j.carbon.2013.11.070
24. Liu YX, Zhang X, Guo L, Wu F (2008) N. S. Deng,Photodegradation of Bisphenol A in the Montmorillonite KSF Suspended Solutions [J],Ind. Eng Chem Res 47:7141–7146. https://doi.org/10.1021/ie800169c

Tables

Table 1 is not available with this version.

Figures

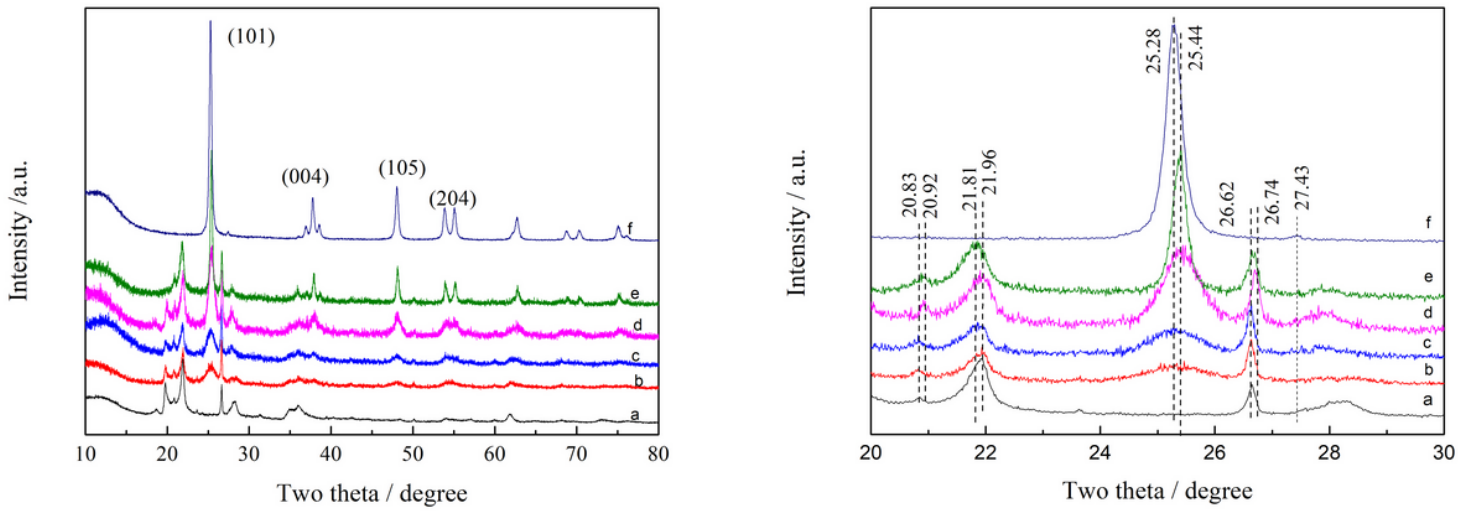

Figure 1

XRD patterns of 30%TiO2/MMT calcined at different temperatures a MMT b 400℃-30%TiO2/MMT c 500℃-30%TiO2/MMT d 600℃-30%TiO2/MMT e 700℃-TiO2/MMT f 600℃-TiO2

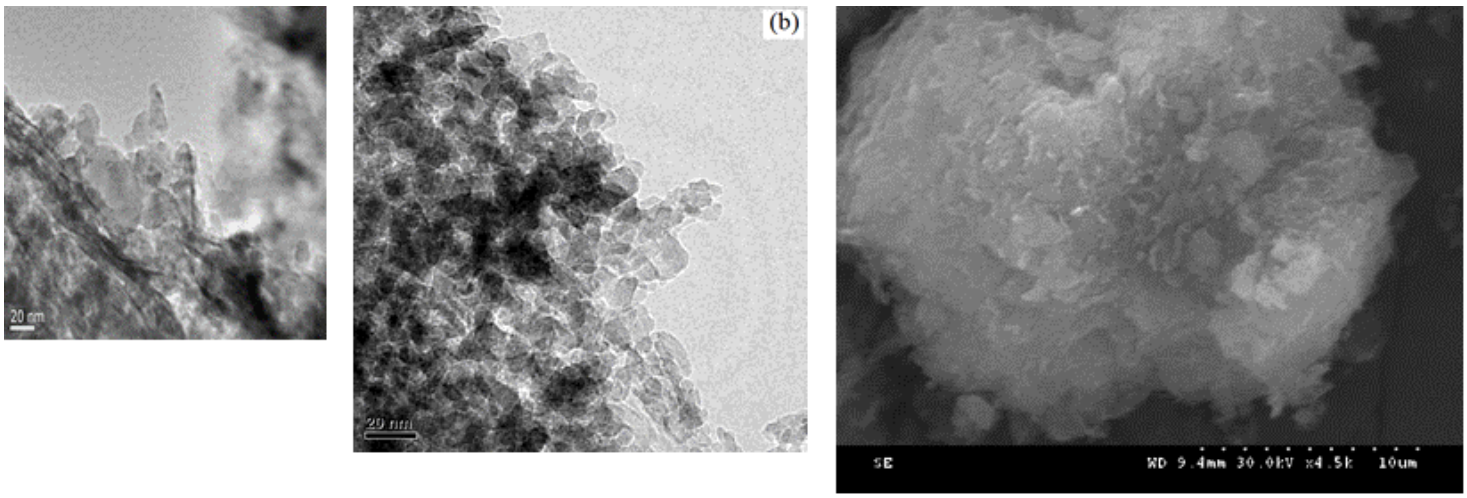

Figure 2

Shows SEM images of raw montmorillonite (a) and TEM images of pure TiO2 (b) and 30% TiO2/MMT (c) composites calcined at 600℃ for 4h

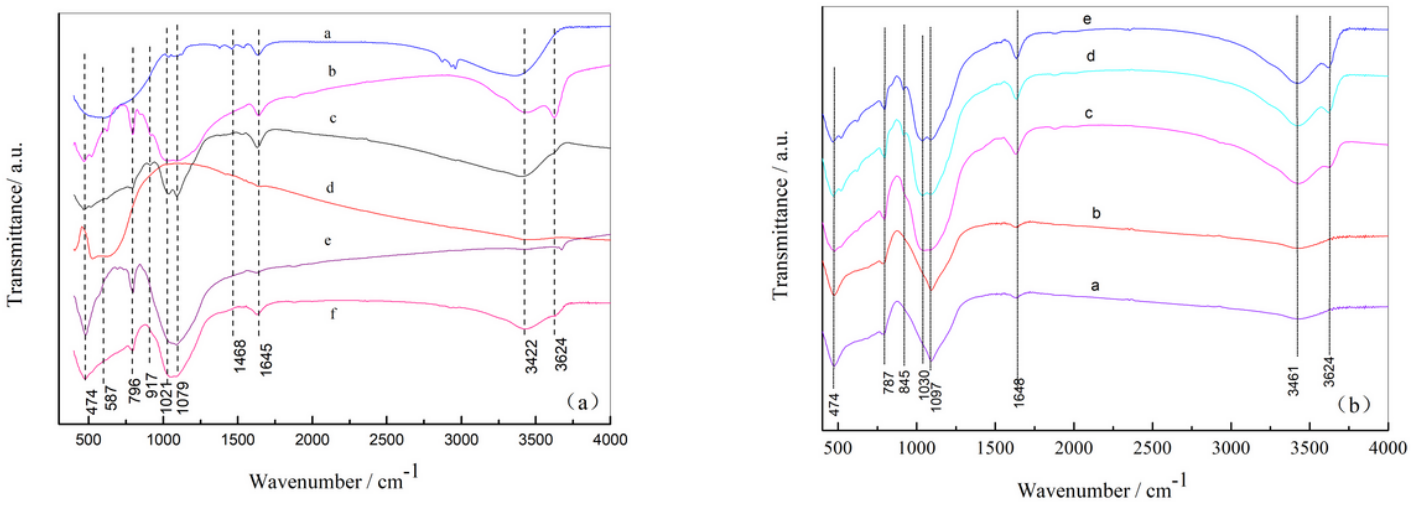

Figure 3

Infrared spectra of each catalyst and composite a 110-TiO2 b 110-MMT c 110-30TiO2 d 600-TiO2 e 600-MMT f 600-30-TiO2-MMT (a) IR spectra of 30% TiO2/MMT Composite (b) IR spectra of 30% TiO2/MMT at different temperatures: a 700℃ b 600℃ c 500℃ d 400℃ e 300℃

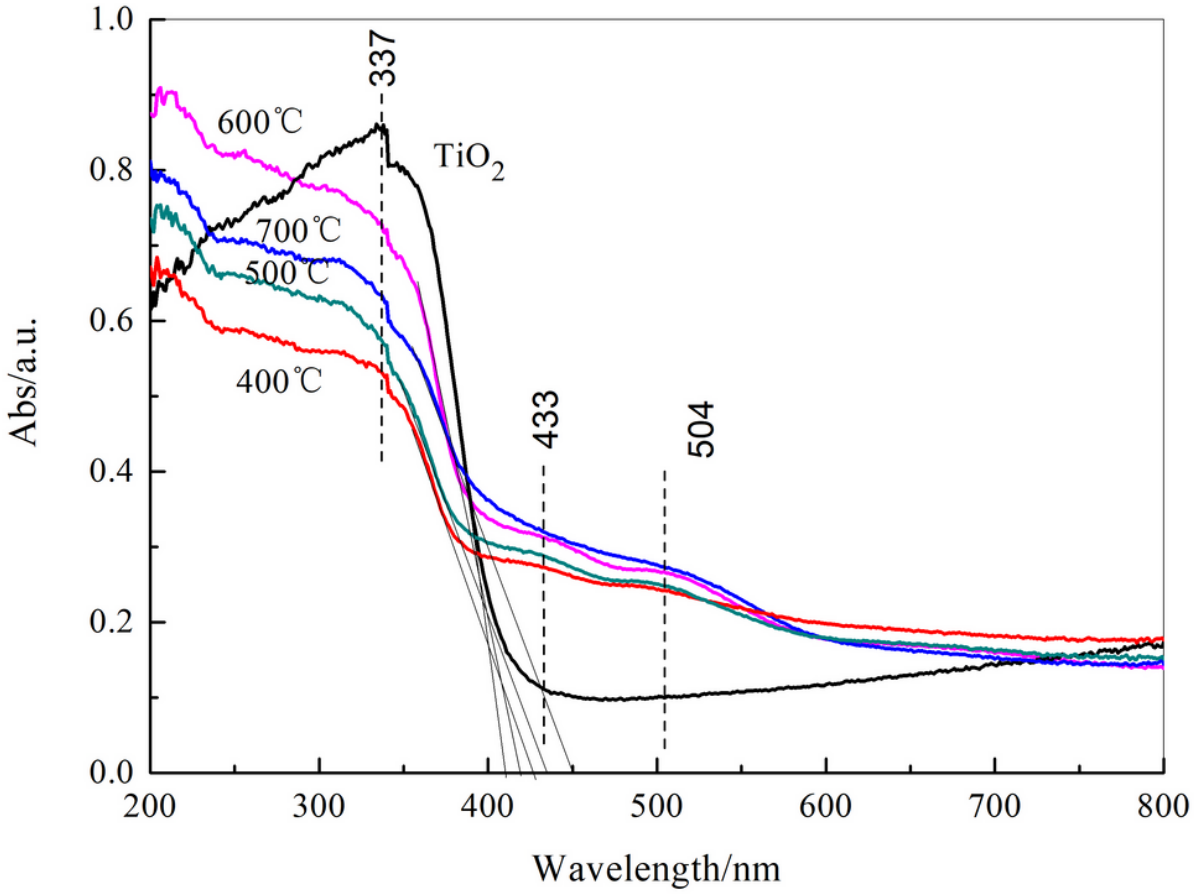

Figure 4

Diffuse reflectance UV-Vis spectra of different sample

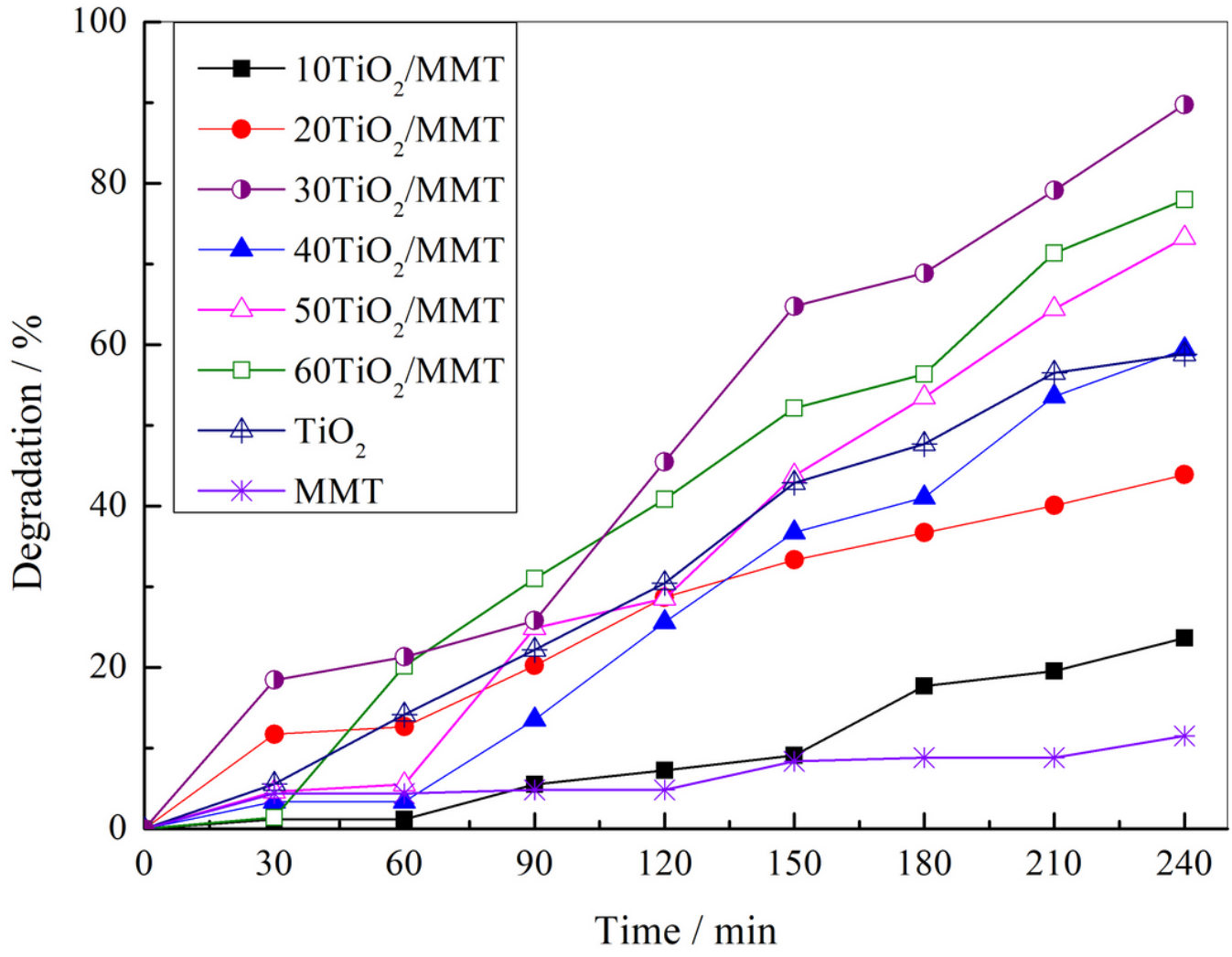

Figure 5

Phenol photocatalytic degradation over different photocatalysts calcined at different temperatures

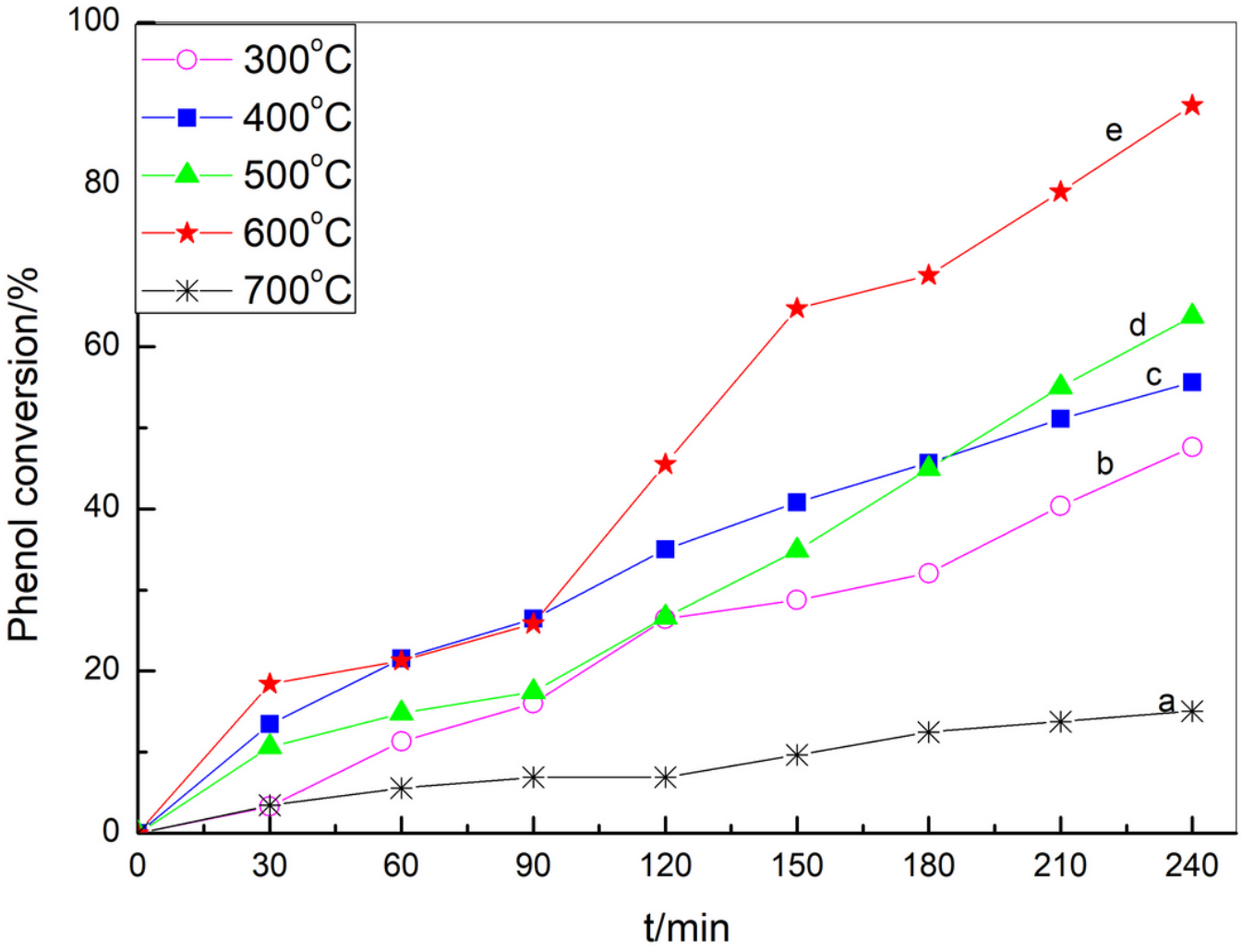

Figure 6

Phenol photocatalytic degradation rate over 30%TiO2/MMT composites calcined at different temperatures

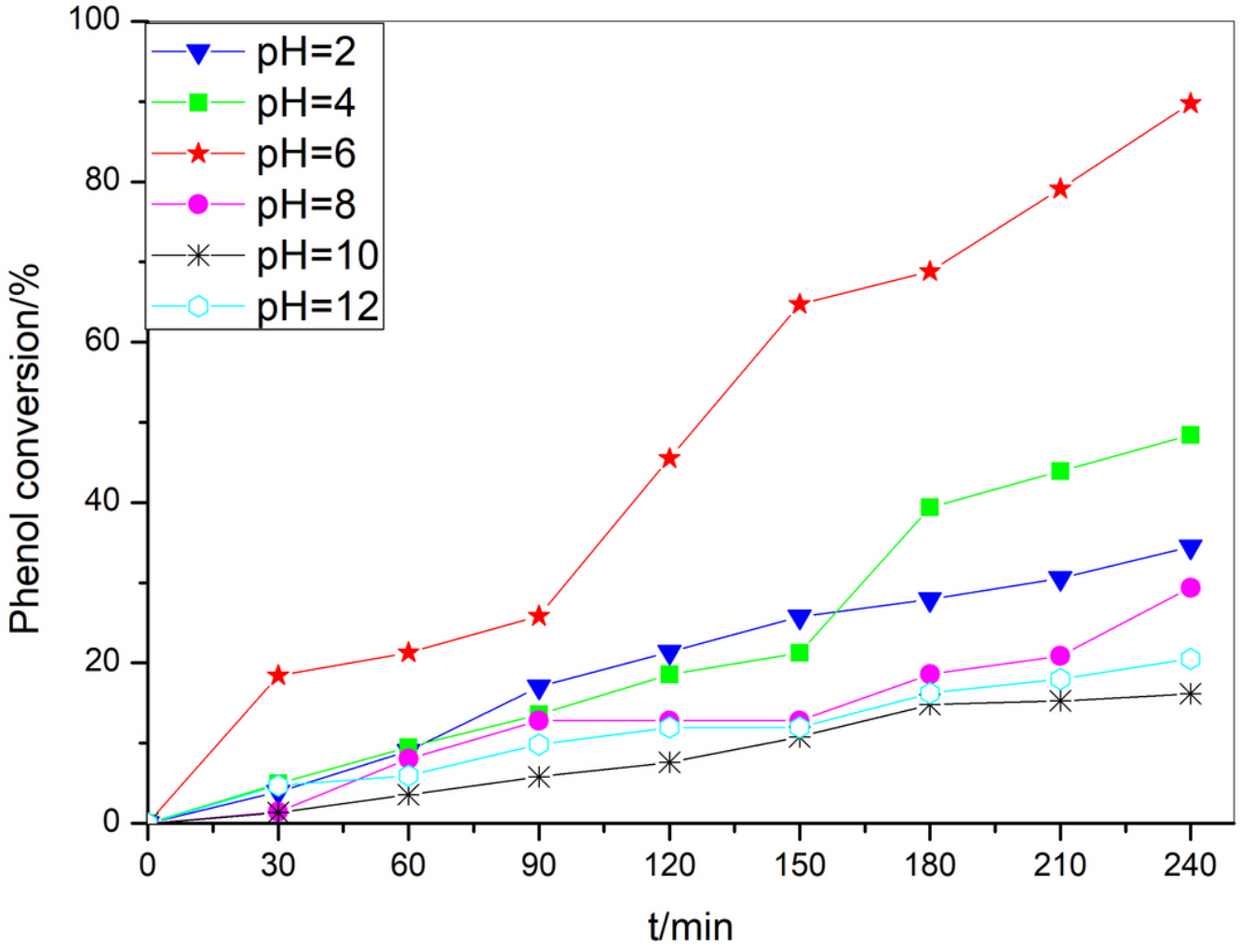

Figure 7

Phenol degradation activity of 30% TiO2/MMT composites in different pH reaction solutions

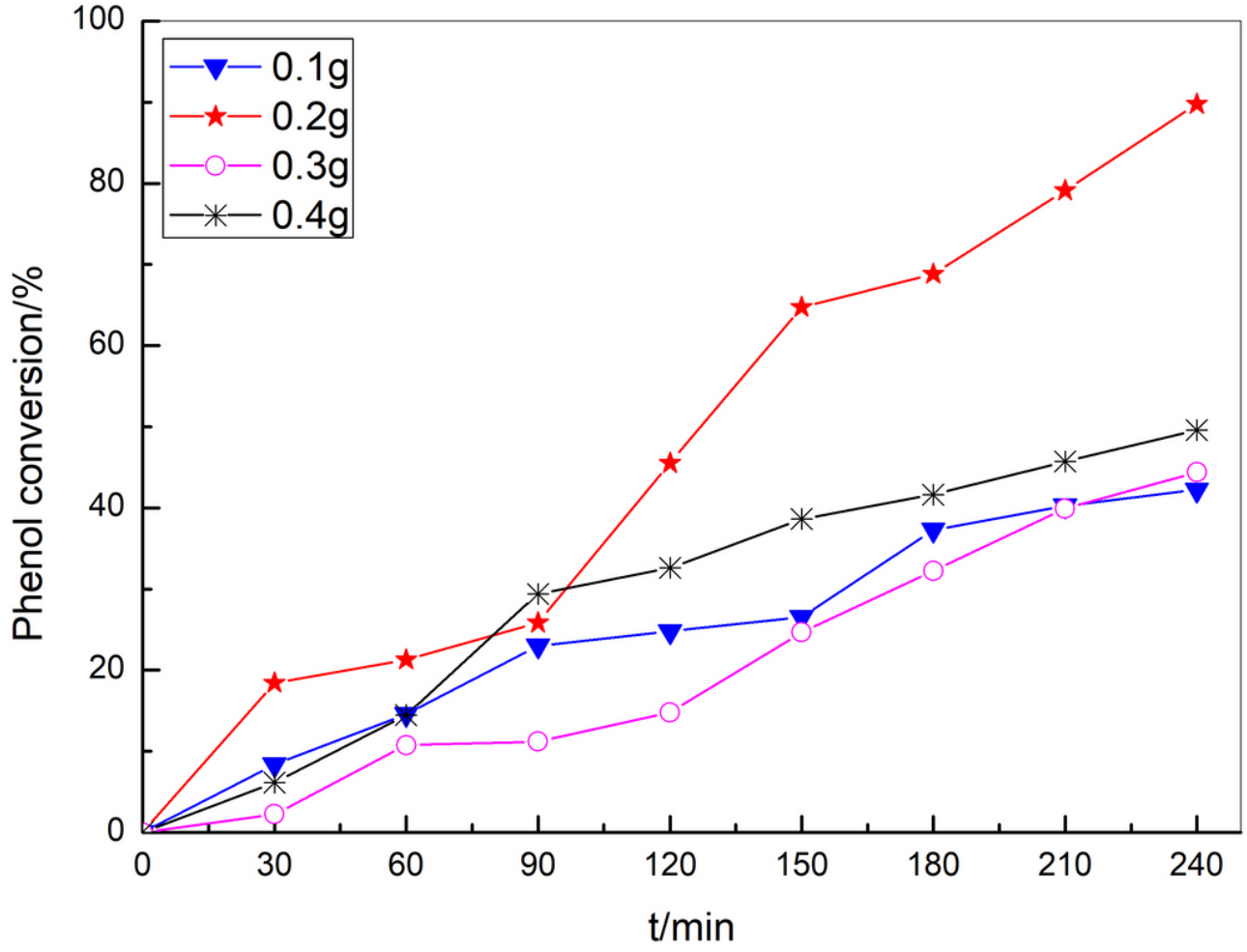

Figure 8

Phenol degradation activity of 30% TiO2/MMT photocatalytic composites with different dosages

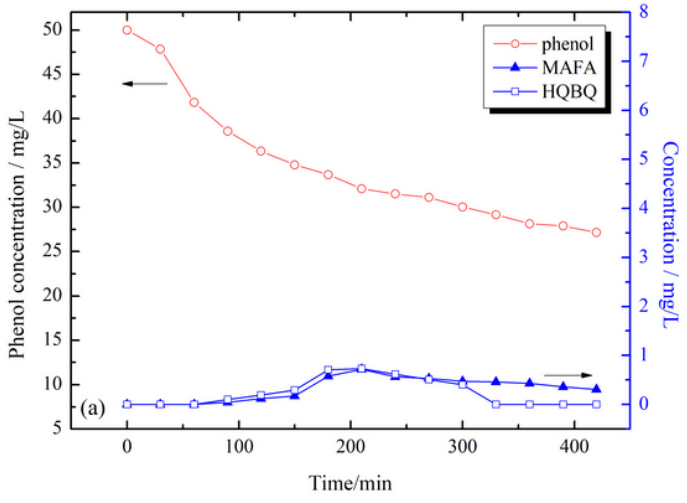

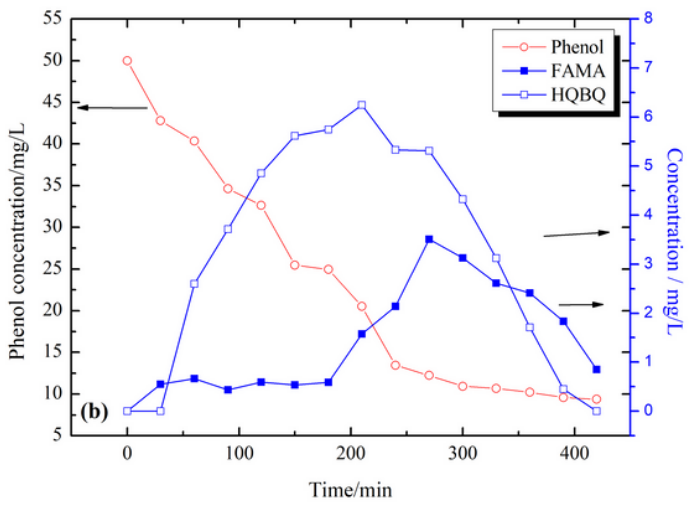

Figure 9

HPLC chromatograms recorded during phenol decomposition under UV light on (a) TiO2 and (b) 30%TiO2/MMT photocatalysts

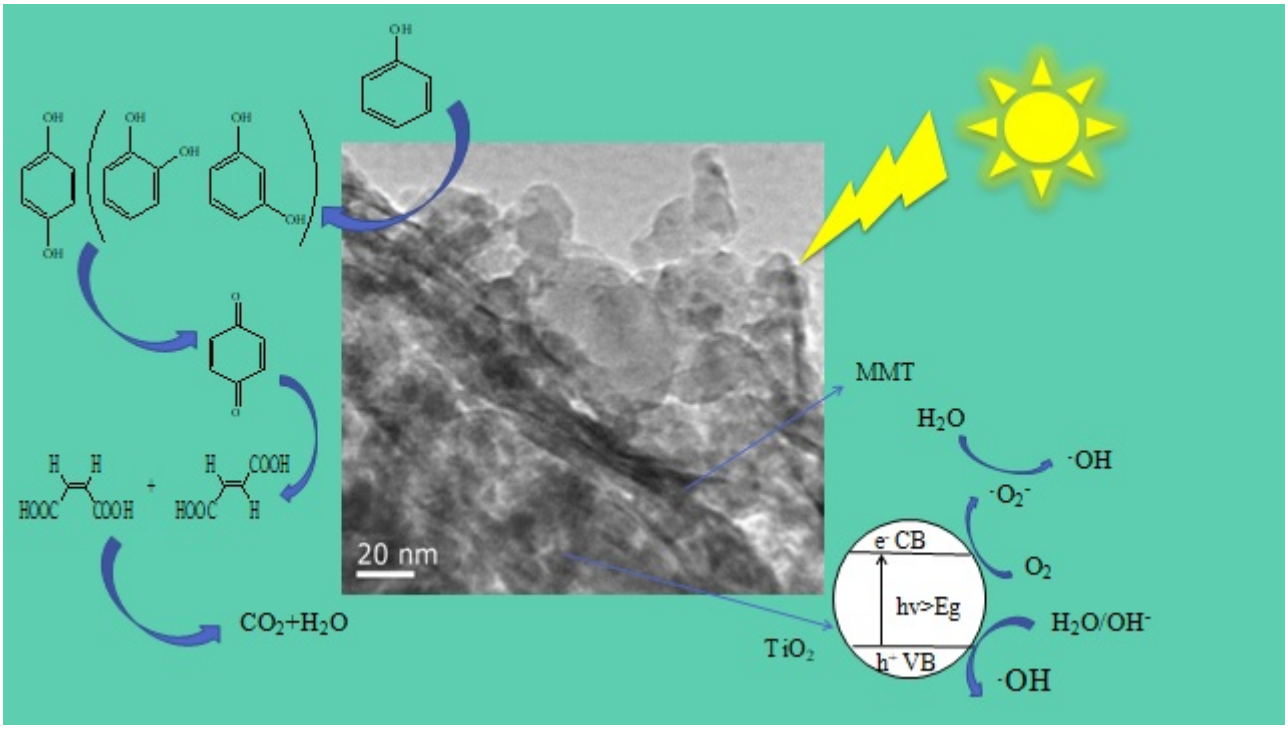

Figure 10

Possible reaction routes for phenol degradation over TiO2/MMT composites

Supplementary Files

This is a list of supplementary files associated with this preprint. Click to download.

- GraphicalAbstract.doc